Carbohydrate Polymers 90 (2012) 650–657

Contents lists available at SciVerse ScienceDirect

Carbohydrate Polymers

journal homepage: www.elsevier.com/locate/carbpol

Infrared study on deuteration of highly-crystalline chitin

Yu Ogawa [a], Satoshi Kimura [a,b], Yukie Saito [a], Masahisa Wada [a,b,*]

[a] Department of Biomaterials Science, Graduate School of Agricultural and Life Sciences, The University of Tokyo, Yayoi 1-1-1, Bunkyo-ku, Tokyo 113-8657, Japan
[b] Department of Plant & Environmental New Resources, College of Life Sciences, Kyung Hee University, 1, Seocheon-dong, Giheung-ku, Yongin-si, Gyeonggi-do 446-701, South Korea

ARTICLE INFO

Article history:
Received 3 April 2012
Received in revised form 22 May 2012
Accepted 24 May 2012
Available online 1 June 2012

Keywords:
α-Chitin
β-Chitin
Deuteration
FT-IR spectroscopy
X-ray diffraction

ABSTRACT

We report an infrared study of the deuteration of highly crystalline α- and β-chitin. With exposure to D_2O vapor, the deuteration of α-chitin progressed on surface molecules, in contrast with β-chitin, which is partially deuterated on the inner part of the crystal. The intracrystalline deuteration occurred with high-temperature annealing in liquid D_2O for α- and β-chitin. In α-chitin, the deuteration was similar between all the three functional groups. The ratio of deuterium/hydrogen increased with treatment temperature, and all the hydrogen in the functional groups was accessible above 200 °C. In β-chitin, the deuteration was more specific for each functional group. The deuteration of O3—H groups progressed rapidly, even below 100 °C, and, by contrast, that of O6—H and N—H progressed relatively slowly. These differences of deuteration between α- and β-chitin presumably arises from the particular ability of β-chitin to form a complex with water molecules.

© 2012 Elsevier Ltd. All rights reserved.

1. Introduction

Chitin is the most abundant biopolymers next to cellulose and is globally widespread. The chemical structure of chitin is based on a linear polymer of β-1,4-linked *N*-acetyl-D-glucosamine (GlcNAc). Similar to cellulose, chitin occurs naturally as crystalline fibrils called microfibrils, and two crystalline polymorphs have been identified: namely, α- and β-chitin.

The crystal structure of α- and β-chitin has been investigated using X-ray diffraction, FT-IR spectroscopy, and solid-state ^{13}C NMR spectroscopy (Blackwell, 1969; Focher, Naggi, Torri, Cosani, & Terbojevich, 1992; Rudall, 1963; Tanner, Chanzy, Vincendon, Roux, & Gaill, 1990). α-Chitin has a two-chains orthorhombic unit cell with $P2_12_12_1$ symmetry, indicating an antiparallel chain arrangement (Fig. 1a) (Minke & Blackwell, 1978; Muzzarelli, 2011; Sikorski, Hori, & Wada, 2009). A molecular sheet in the *ac*-plane where all chains aligned in the same direction, parallel fashion, is formed by hydrophobic interaction of glucopyranoside rings and by intermolecular hydrogen bonds. The sheets having different polarity are alternately stacked along the *b*-axis direction to form an antiparallel structure, and the stacking sheets are stabilized with intermolecular hydrogen bonds between the sheets. Originating from this structural feature where hydrogen bonds exist within and between the molecular sheets, α-chitin is more thermodynamically stable than the β-chitin polymorph.

On the other hand, it is known that an anhydrous form and at least two hydrate forms exist for β-chitin. The anhydrous β-chitin has a one-chain monoclinic unit cell, with $P2_1$ symmetry, and consists of a parallel chain arrangement (Fig. 1b) (Gardner & Blackwell, 1975; Nishiyama, Noishiki, & Wada, 2011; Sawada et al., 2012). Anhydrous β-chitin also has a similar molecular sheet structure to α-chitin in the *ac*-plane. However, these sheets having the same polarity are stacked because of hydrophobic forces to form a parallel structure, and thus no strong hydrogen bond exists between the sheets along the *b*-axis. Because of the lack of hydrogen bonds between its sheets, β-chitin has the ability to incorporate small molecules, such as water, primary alcohols, and amines, between its sheets (Blackwell, 1969; Noishiki, Kuga, Wada, Hori, & Nishiyama, 2004; Saito, Okano, Gaill, Chanzy, & Putaux, 2000). The crystal structures of β-chitin hydrates, dihydrate and monohydrate forms, have not been well understood, but must have a parallel chain arrangement similar to that found in the anhydrous form because of the reversibility of its water molecule complexes (Kobayashi, Kimura, Togawa, & Wada, 2010; Saito, Kumagai, Wada, & Kuga, 2002).

In comparison with cellulose, the utilization of chitin is quite limited despite its abundance. To promote its utilization, it is quite important to investigate the property–structure relationships of chitin. Recently, thermal expansion and elastic modulus in the crystalline region have been studied with X-ray diffraction analyses (Ogawa, Hori, Kim, & Wada, 2011a; Wada & Saito, 2001), but its chemical activities and affinities should be further investigated

* Corresponding author at: Department of Biomaterials Science, Graduate School of Agricultural and Life Sciences, The University of Tokyo, Tokyo 113-8657, Japan. Tel.: +81 3 5841 5247; fax: +81 3 5841 2677.
E-mail address: awadam@mail.ecc.u-tokyo.ac.jp (M. Wada).

0144-8617/$ – see front matter © 2012 Elsevier Ltd. All rights reserved.
http://dx.doi.org/10.1016/j.carbpol.2012.05.092

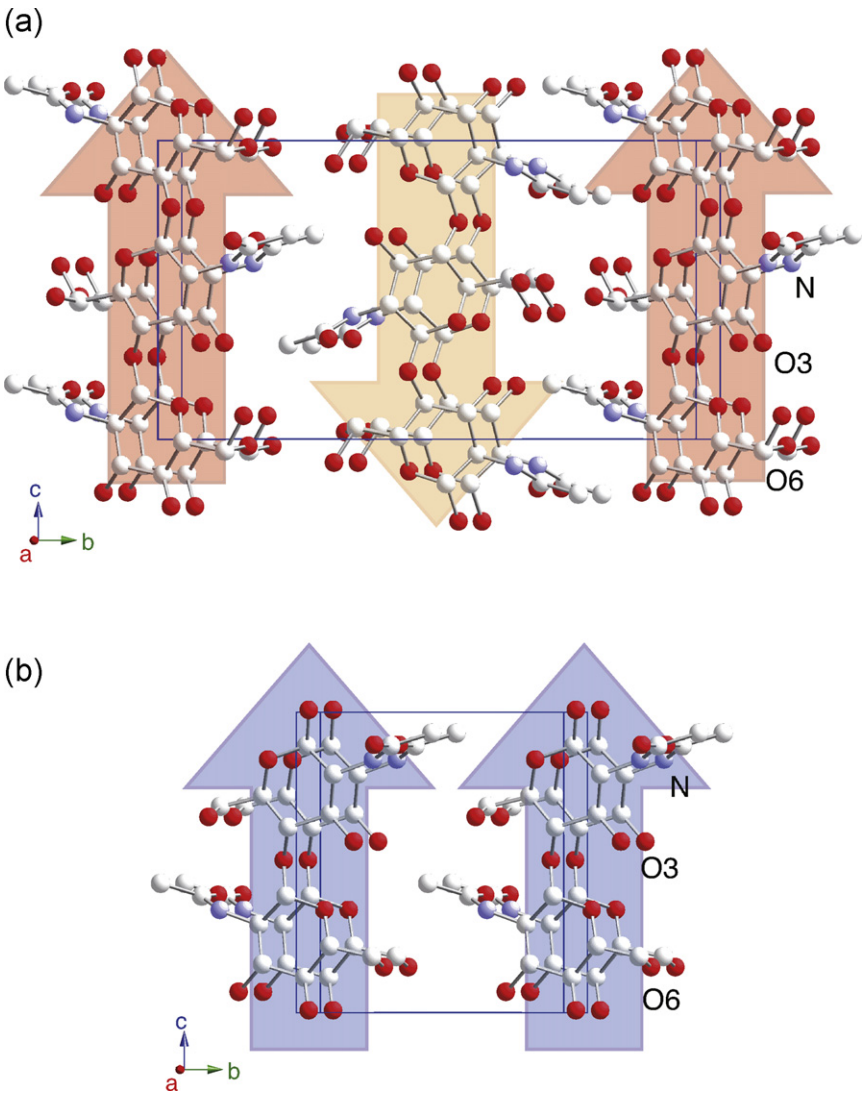

Fig. 1. Crystal structure of (a) α-chitin (Sikorski et al., 2009), and (b) β-chitin (Nishiyama et al., 2011). The molecular sheets are denoted as colored arrows pointing to the reducing ends of chitin molecules. (For interpretation of the references to color in this figure legend, the reader is referred to the web version of the article.)

because they are also important properties that correlate with its structure.

Deuterium has been used as useful chemical reagent to estimate an influence to substrates from chemical external forces. Hydrogen in functional groups, such as hydroxyl and amino groups can be exchanged reversibly by deuterium when the substrates are mixed with D_2O. This phenomenon, namely deuteration can also occur on the polymers with the ordered structure, but is hard to progress on the inner molecules of the structure due to the resistance from molecular interactions. Such accessibility of each functional group should reflect the higher-order structure of the polymers. Thus, there are many studies of the deuteration of various polymers such as DNA, starch, cellulose, and synthetic polymers (Frilette, Hanle, & Mark, 1948; Mann & Marrinan, 1956a, 1956b; Nara, Takeo, & Komiya, 1981; Tadokoro, Seki, & Nitta, 1956). Especially for native cellulose, the deuteration technique has been well developed to investigate crystalline and surface regions of the microfibril. On the surface of cellulose, deuteration immediately progresses with simple soaking in D_2O or exposure to D_2O vapor at room temperature (Mann & Marrinan, 1956a). Conversely, the crystalline region of cellulose is almost inaccessible at room temperature. Intracrystalline deuteration can be achieved by high-temperature annealing in D_2O without any change in its crystalline phase (Nishiyama, Isogai, Okano, Mueller, & Chanzy, 1999; Wada, Okano, and Sugiyama, 1997). Because deuterium has different scattering properties to hydrogen, intracrystalline deuterated samples have been used for neutron diffraction studies to analyze the hydrogen-bonding system of cellulose (Nishiyama, Langan, & Chanzy, 2002; Nishiyama, Sugiyama, Chanzy, & Langan, 2003; Nishiyama, Johnson, French, Forsyth, & Langan, 2008).

Deuteration studies have also been conducted on other cellulose polymorphs (Jefferies, 1963; Langan, Nishiyama, & Chanzy, 1999; Marrinan & Mann, 1956; Valentin, Bonelli, Garrone, Di Renzo, & Quingnard, 2007; Wada, Chanzy, Nishiyama, & Langan, 2004). However, to our knowledge, there are only a few studies of deuteration of chitin polymorphs. In one study, α-chitin from lobster was deuterated by D_2O vapor at room temperature and investigated by FT-IR measurement to assign each band of the spectrum (Pearson, Marchessault, & Liang, 1960). In other studies, the deuteration of highly crystalline β-chitin was conducted by either immersing it in D_2O or CH_3OD or concentrated DCl in D_2O to analyze the swelling of β-chitin (Saito et al., 2000; Saito, Tomotake, and Shida, 2007). In these studies, partial intracrystalline deuteration occurred, but complete deuteration could not be achieved under the conditions used. To our knowledge, no study published so far has focused on differences of deuteration between α- and β-chitin.

In this study, therefore, α- and β-chitin, with almost the same crystallite sizes, were subject to deuteration by D_2O vapor and liquid at room temperature. Intracrystalline deuteration was also conducted on the two polymorphs using the same high-temperature annealing method as used for cellulose, and differences in intracrystalline deuteration with treatment temperature were compared between these two polymorphs.

2. Materials and methods

2.1. Sample preparation

Phaeocystis globosa (NIES-1396) were obtained from the National Institute for Environmental Studies (Tsukuba, Japan) and cultured in mIMR medium at 20 °C with aeration under 12 h light–dark cycles of 100 μmol photons m^{-2} s^{-1} for about one month. The suspended solid in the medium was collected by centrifugation, and the precipitate was purified by the methods reported previously (Ogawa, Kimura, Wada, & Kuga, 2010). Purified chitin was freeze-dried and kept in a desiccator.

Satsuma tubeworms (*Lamellibrachia satsuma*) were collected from Kagoshima Bay, Japan, at a depth of about 100 m, using a remotely operated vehicle (Hyper-Dolphin; JAMSTEC, Japan). The bodies of the tubeworms were removed by washing the tubes with water. The tubes were purified using a repetitive treatment employing 5% KOH and 0.3% $NaClO_2$ solutions, as described previously (Ogawa, Kimura, & Wada, 2011b). The purified chitin was freeze-dried and kept in a desiccator.

2.2. X-ray diffraction analysis

X-ray diffractometry was conducted in reflection mode (RINT2000, Rigaku, Japan), with monochromatic Cu Kα radiation (λ = 1.5418 Å), generated at 38 kV and 50 mA using an optical slit system: divergence slit = 0.5°; scattering slit = 0.5°; and receiving slit = 0.3 mm. Scanning was performed using the following settings: scattering angle, 2θ = 5–30° with a 2θ step of 0.05° and accumulation time of 20 s.

To measure the diffraction spectra of the anhydrous and the hydrated forms, β-chitin samples were prepared using three different procedures. The anhydrous sample was prepared from a dried sample over P_2O_5 in a desiccator after freeze-drying. The monohydrated and dihydrate β-chitin samples were prepared according to the method described by Kobayashi et al. (2010). The monohydrated sample was prepared from anhydrous β-chitin by exposure to water vapor (R.H. 100%) in a desiccator at room temperature. The dihydrate sample was prepared also from anhydrous β-chitin, by soaking it in water. After soaking, the wet sample was stored in a desiccator with saturated KCl aqueous solution (R.H. 85%) to remove the excess water. Measurements on both hydrated forms were conducted under 1 L/min of humidity-controlled airflow (R.H. 100%) provided by a humidity generator (Shinyei SRG-1R) to avoid desiccation.

The peak positions were determined by peak separation of the X-ray diffraction spectra using a non-linear least-squares-fitting program for pseudo-Voigt function, and crystallite sizes were estimated by substituting the value for full-width at half-maximum (FWHM) into the Scherrer equation (Alexander, 1979; Wada et al., 1997).

2.3. Deuteration and FT-IR spectroscopy

Deuteration of chitin samples was achieved with both vaporous and liquid D_2O. For vapor-phase deuteration, the dried thin films of purified chitin were exposed to D_2O vapor at 100% R.H. and 25 °C in a desiccator for specified times (1 h, and 24 h), and dried in vacuo at 25 °C. For liquid-phase deuteration, the purified chitin samples were annealed in 0.1 N NaOD–D_2O solution for 60 min at various temperatures, ranging from 25 °C to 260 °C. After rinsing with D_2O, the treated samples were dried onto PTFE sheets in vacuo at 25 °C to form thin films.

The primary and crystal structure of chitin before/after the deuteration was analyzed with elementary analysis and X-ray diffraction, and it was confirmed that major structural change such as deacetylation did not occur through the deuteration treatment, except in hydrogen atoms (data not shown).

FT-IR spectra of chitin samples were recorded with 4 cm^{-1} resolution and 64 scans on a Nicolet Magna 860 (Madison, WI, USA) in transmission mode, and analyzed with OMNIC software (Thermo scientific, Waltham, MA, USA). The spectra were normalized using the 2900 cm^{-1} band in the C—H stretching region as an internal standard. The ratio of deuterium/hydrogen, R_D at each functional group, O6—H, O3—H, and N—H, were estimated using the following equation:

$$R_D = \frac{\alpha A_D}{\alpha A_D + A_H}, \quad (1)$$

where A_D is absorbance of O—D and N—D stretching bands, and A_H is absorbance of a corresponding O—H and N—H stretching band, and α is a corrective coefficient estimated from the ratio of the molar extinction coefficient between O—D and O—H stretching bands, and between N—D and N—H stretching bands: 1.11 for O—D/O—H stretching bands (Mann & Marrinan, 1956b) and N—D 1.41 for N—D/N—H stretching bands (Shih, Yeh, Lee, & Yang, 2001), respectively.

3. Results and discussion

3.1. X-ray diffraction analysis

Fig. 2a andb shows the X-ray diffraction spectra of α-chitin from *Phaeocystis* and anhydrous β-chitin from *Lamellibrachia*. Both profiles have sharp diffraction peaks indicating their large crystallite sizes. Four reflections on each profile could be indexed according to proposed crystalline models: two chains of an orthorhombic unit cell for α-chitin (Sikorski et al., 2009) and a one-chain monoclinic unit cell for anhydrous β-chitin (Nishiyama et al., 2011). The crystallite sizes corresponding to width of microfibrils of α-chitin and anhydrous β-chitin were calculated using 0 2 0 and 0 1 0 diffractions, respectively. The (0 2 0) and (0 1 0) directions correspond to the stacking direction of the molecular sheets that are a common structure of α-chitin and β-chitin (Ogawa et al., 2011b). The crystallite sizes of both crystals calculated with the Scherrer equation are nearly equal; the values are 18.2 nm for α-chitin and 19.0 nm for anhydrous β-chitin. Therefore, differences in deuteration between these two samples described below should be derived almost entirely from their crystal structures.

Fig. 2c is the X-ray diffraction spectrum of β-chitin from *Lamellibrachia* that was exposed to moisture and is consistent with that of the monohydrate β-chitin reported previously (Kobayashi et al., 2010). Therefore, with exposure to water vapor, the anhydrous β-chitin was converted to a monohydrate β-chitin form by intercalation of water molecules. Fig. 2d is the X-ray diffraction spectrum of β-chitin that was soaked in water and corresponds to dihydrate β-chitin. Thus, the anhydrous β-chitin was converted to a dihydrate form upon soaking in liquid water. Both of these hydrated β-chitin forms were reversibly converted to the anhydrous form by drying (data not shown). However, the crystal structure of α-chitin is stable in the presence of water.

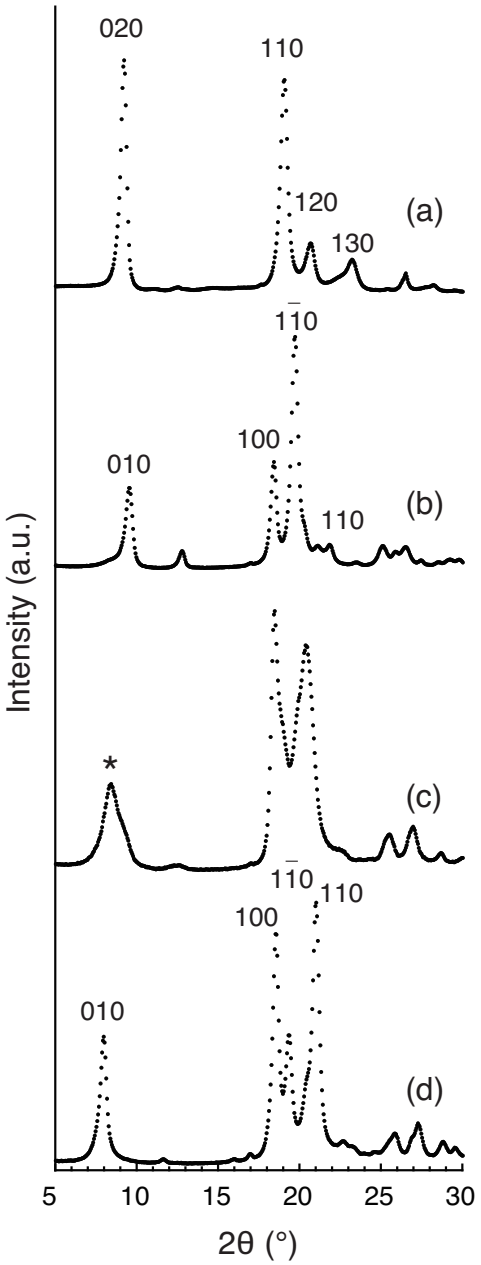

Fig. 2. X-ray diffraction spectra of (a) α-chitin from *Phaeocystis*, (b) anhydrous, (c) monohydrated, and (d) dihydrate β-chitin from *Lamellibrachia*. The indices are shown upon each diffraction pattern. The asterisk (*) denotes the characteristic reflection of monohydrated β-chitin with *d* spacing = 10.4 Å.

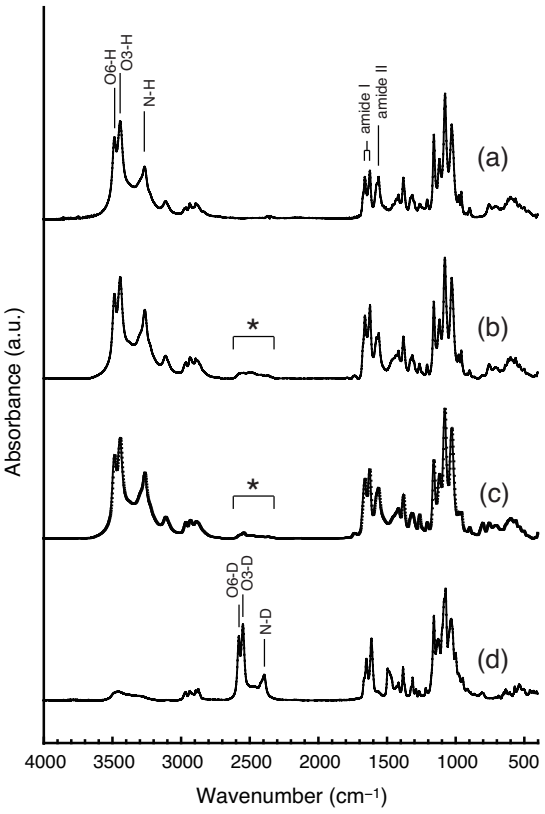

Fig. 3. FT-IR spectra of α-chitin before and after deuteration. (a) Initial, untreated α-chitin. (b) α-Chitin after exposure to vaporous D_2O at 25 °C for 1 h. The asterisk (*) denotes the new band resulting from vapor deuteration. (c) α-Chitin after soaking in D_2O at 25 °C for 1 h. The asterisk (*) denotes the new band resulting from vapor deuteration. (d) α-Chitin after annealing in liquid D_2O at 260 °C for 1 h.

3.2. Deuteration of α-chitin

Figs. 3 and 4 show FT-IR spectra of α-chitin before and after deuteration.

The spectrum of untreated α-chitin (Fig. 3a) shows the typical features of α-chitin, such as a doublet amide I band at 1655 and 1661 cm^{-1}, a singlet amide II band at 1550 cm^{-1}, and three definite bands in the high wavenumber region assigned as N—H stretching at 3260 cm^{-1}, O3—H stretching at 3441 cm^{-1}, and O6—H stretching vibrations at 3482 cm^{-1}, respectively (Sikorski et al., 2009). The spectrum is well resolved in comparison with those of crustacean and insect α-chitin indicating the high crystallinity of α-chitin from *Phaeocystis* (Ogawa et al., 2010).

The spectrum of α-chitin after exposure to D_2O vapor for 1 h at 25 °C (Figs. 3b and 4) shows almost the same features as the untreated α-chitin, but a broad and weak band is observed at the region from 2350 to 2650 cm^{-1}. Because this region corresponds to O—D and N—D stretching vibration, partial deuteration of O—H and N—H groups occurred after exposure to D_2O vapor. However, this band is much broader than any other band in the spectrum, and the ratio of deuterium/hydrogen R_D was below 0.05 for all the functional groups. This finding indicated that the deuteration effected by D_2O vapor only occurs on the surface molecules of the microfibrils. The absorbance of O—D and N—D bands did not increase after exposing the sample to D_2O vapor for 24 h (data not shown). In a previous study, however, an efficient intracrystalline deuteration of α-chitin from lobster was achieved by its exposure to D_2O vapor and the R_D value was over 0.5. This difference might be the result of differences in the crystallinity of the samples and the pretreatment with DCl in the previous study (Pearson et al., 1960).

The spectrum of α-chitin after soaking in D_2O for 1 h at 25 °C (Figs. 3c and 4) shows almost the same features as that after vapor deuteration. Thus, the deuteration progressed only on the surface molecules of α-chitin under these conditions, as was also seen after the vapor deuteration.

On the other hand, after high-temperature annealing at 260 °C in liquid D_2O, the spectrum of deuterated α-chitin was changed dramatically from that of initial α-chitin (Figs. 3d and 4). The sharp O—H and N—H stretching bands located at around 3100–3500 cm^{-1} were almost completely shifted to the lower wavenumber region at around 2300–2600 cm^{-1} without loss of sharpness. These sharp O—D and N—D stretching bands could be assigned as N—D at 2389 cm^{-1}, O3—D at 2542 cm^{-1}, and O6—D stretching at 2575 cm^{-1} (Pearson et al., 1960). Therefore, the intracrystalline deuteration of α-chitin progressed into the entire crystalline region under these

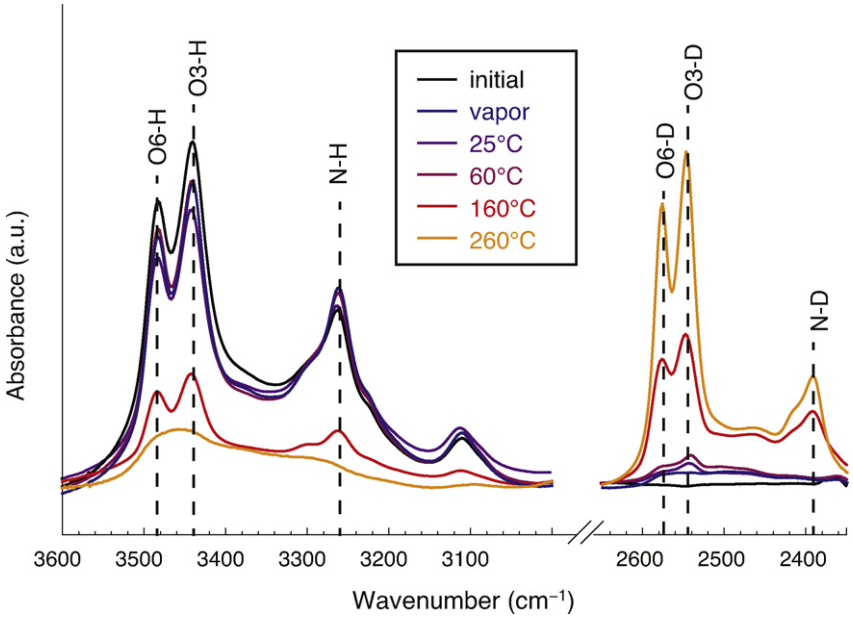

Fig. 4. O—H, N—H and O—D, N—D stretching regions of FT-IR spectra of α-chitin after deuteration at various temperatures. Assigned bands are indicated with dashed lines.

conditions. Moreover, despite the unchanged amide I bands, mainly associated with C=O stretching vibration, the amide II bands, associated with both N—H bending and C—N stretching, almost disappeared. These bands should also shift to a lower wavenumber region because of the deuteration of N—H to N—D, but might overlap the fingerprint region below 1000 cm^{-1}.

To analyze the deuteration of α-chitin, high-temperature annealing in liquid D_2O was conducted at various temperatures. Fig. 4 shows a series of FT-IR spectra of α-chitin after deuteration at various treatment temperatures. With increasing temperature, the absorbance of O—H and N—H stretching bands decreased and the absorbance of the O—D and N—D stretching bands increased. The changes in the R_D for each functional group with temperature are shown in Fig. 5. The deuteration changes with increasing temperature were similar between three functional groups, O3—H, O6—H, and N—H. Below 100 °C, the R_D values gradually increased up to 0.1, indicating that almost all surface molecules were deuterated. From 120 °C to 180 °C, the R_D values increased dramatically, indicating that the portion of the molecules in the inner part of crystal were accessible. Above 200 °C, the R_D value had almost plateaued at 0.8, indicating that almost all the molecules in the crystal were accessible.

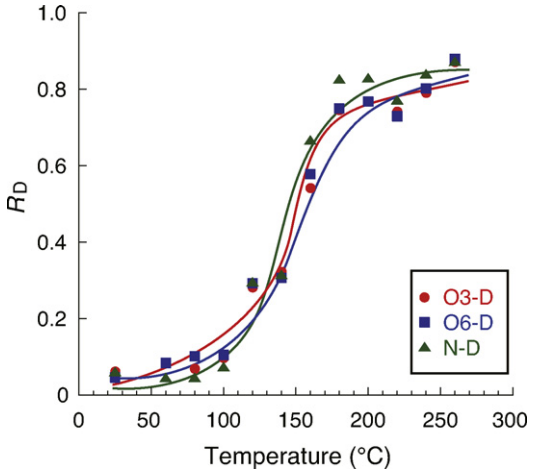

Fig. 5. Changes in the ratio of deuterium/hydrogen, R_D, of each functional group of α-chitin, with temperature.

The increase in the accessibility of molecules for deuteration with temperature, observed in α-chitin, was also observed in native cellulose (cellulose I). Horikawa and Sugiyama reported that a rapid exchange between deuterium and hydrogen occurred above 170 °C (Horikawa & Sugiyama, 2008). After two-dimensional FT-IR spectroscopy, Kokot et al. independently reported that the intermolecular hydrogen bonding in a cellulose I crystal would break down above 150 °C (Kokot, Czamik-Mautusewicz, & Ozaki, 2002). Thus, the cleavage of hydrogen bonds in the crystal was associated with increased accessibility of cellulose molecules. The same explanation could be applied to α-chitin. The rapid deuteration of α-chitin beginning at 120 °C is likely caused by the lower thermodynamic stability of α-chitin compared with that of cellulose I (Hori & Wada, 2005; Ogawa et al., 2011a; Wada, 2002; Wada & Saito, 2001).

3.3. Deuteration of β-chitin

Figs. 6 and 7 show FT-IR spectra of β-chitin before and after deuteration.

The spectrum of untreated β-chitin (Fig. 6a) shows the typical features of anhydrous β-chitin crystals, such as a singlet amide I band at 1627 cm^{-1}, an amide II band at 1557 cm^{-1}, and three definite bands in the high wavenumber region of its spectrum, assigned as N—H stretching at 3292 cm^{-1}, O3—H stretching at 3438 cm^{-1}, and O6—H stretching vibrations at 3462 cm^{-1} (Saito & Iwata, 2012). Similar to the spectrum of α-chitin from *Phaeocystis*, that of β-chitin from *Lamellibrachia* is well resolved, indicating its high crystallinity.

After exposure to D_2O vapor for 1 h at room temperature, the spectrum still shows (Figs. 6b and 7) strong O—H and N—H bands at the same positions as those of anhydrous β-chitin and weak, but sharp, bands in O—D stretching regions were observed, in contrast to the blurred deuterated bands of α-chitin after deuteration in D_2O vapor (Fig. 3b). Therefore, the deuteration progressed slightly on the inner part of the β-chitin crystal. In D_2O vapor, the β-chitin crystal was converted to a monohydrated form with D_2O molecules, as shown by X-ray diffraction analysis. Therefore, this partial intracrystalline deuteration is probably the result of its conversion into the monohydrated form. At room temperature, the deuteration under D_2O vapor did not progress further with time

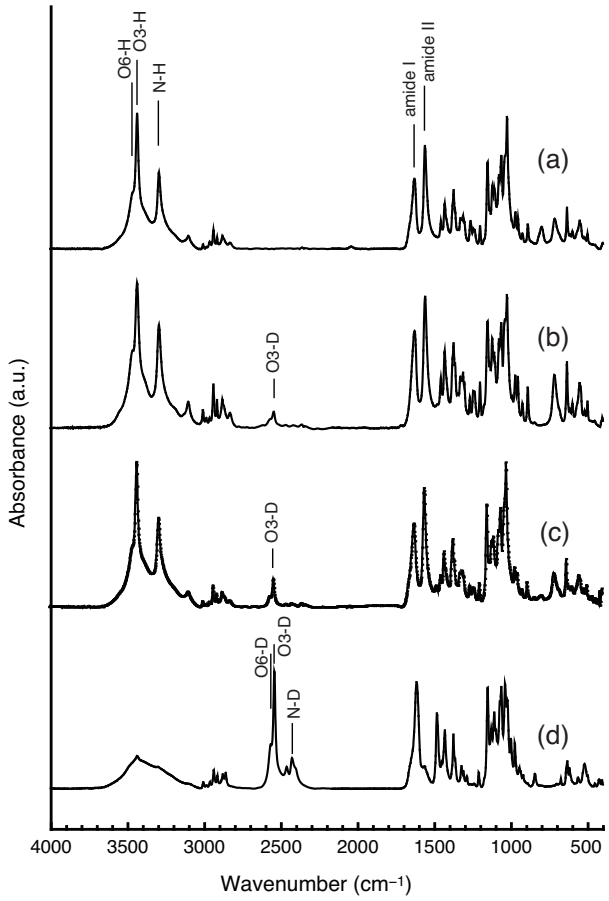

Fig. 6. FT-IR spectra of β-chitin before and after deuteration. (a) Initial, untreated β-chitin. (b) β-Chitin after exposure to vapor D_2O at 25 °C for 1 h. (c) β-Chitin after soaking in D_2O at 25 °C for 1 h. (d) β-Chitin after annealing in liquid D_2O at 160 °C for 1 h.

(data not shown); thus, the exchange between the hydrogen of β-chitin and deuterium of guest D_2O molecules is probably limited at room temperature.

The spectrum of β-chitin after soaking in D_2O for 1 h at 25 °C is shown in Figs. 6c and 7. Only after soaking in D_2O at 25 °C are the sharp O3—D and O6—D bands observed. In liquid D_2O the β-chitin crystal should be in a dihydrate form; thus, the exchange between hydrogen and deuterium on O3 and O6 groups occurred relatively easily with guest D_2O molecules. In contrast, an N—D stretching band was barely observed with this condition. The geometric states between each functional group and the D_2O water molecules might affect deuteration; in the dihydrate form, the N—H group would therefore be situated away from guest D_2O molecules compared with the O—H groups. The exchange at O3 and O6 groups would still be limited in dihydrate form at room temperature, because there was no change in the spectrum of β-chitin after treatment in D_2O for several days (data not shown).

After high-temperature annealing at 160 °C in liquid D_2O intracrystalline, deuteration also occurred as found for α-chitin. In the deuterated β-chitin spectrum (Figs. 6d and 7), the sharp O—H and N—H stretching bands located around 3100–3500 cm^{-1} were almost completely shifted to a lower wavenumber region around 2300–2600 cm^{-1} without loss of resolution. These sharp O—D and N—D stretching bands could be assigned as N—D at 2425 cm^{-1}, O3-D at 2541 cm^{-1}, and O6—D stretching at 2468 cm^{-1}, as in the previous study (Saito et al., 2000). The sharp band observed at 2460 cm^{-1} might be associated with N—D stretching, but such assignment was not conclusive in this study. The amide II band also disappeared because of deuteration of N—H to N—D, as found for α-chitin.

To analyze the deuteration of β-chitin, high-temperature annealing in liquid D_2O was conducted at various temperatures. Fig. 7 shows the series of β-chitin FT-IR spectra after deuteration at various treatment temperatures. As found for α-chitin, the absorbance of O—H and N—H stretching bands decreased with increasing temperature. However, the absorbance of O—D and N—D did not show the same tendency with temperature. The absorbances of these bands for β-chitin treated at 260 °C were weaker than those at 160 °C, and almost the same as those at 60 °C. A possible explanation is that heat degradation of β-chitin occurring around 260 °C caused a decrease of these absorbances. The

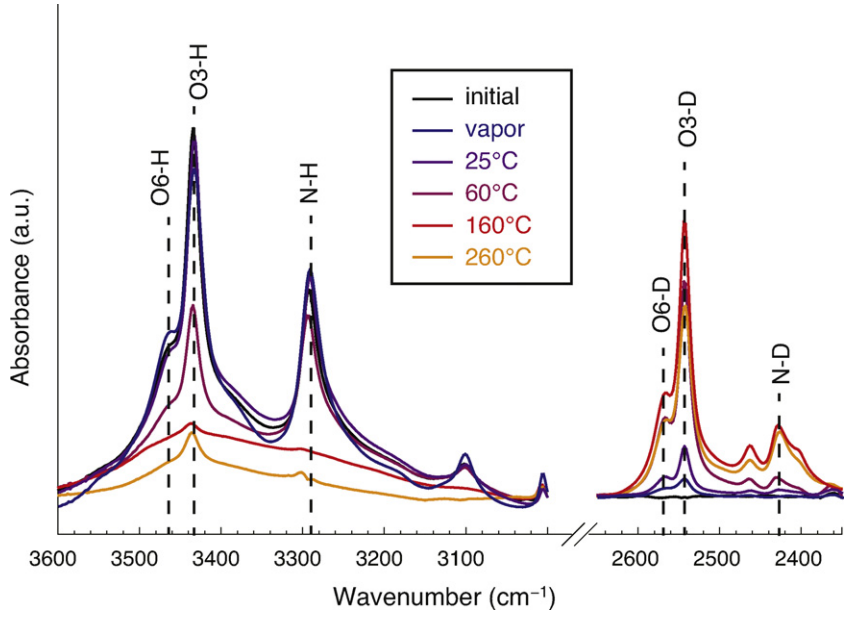

Fig. 7. O—H, N—H and O—D, N—D stretching regions of FT-IR spectra of β-chitin after deuteration at various temperatures. Assigned bands are indicated with dashed lines.

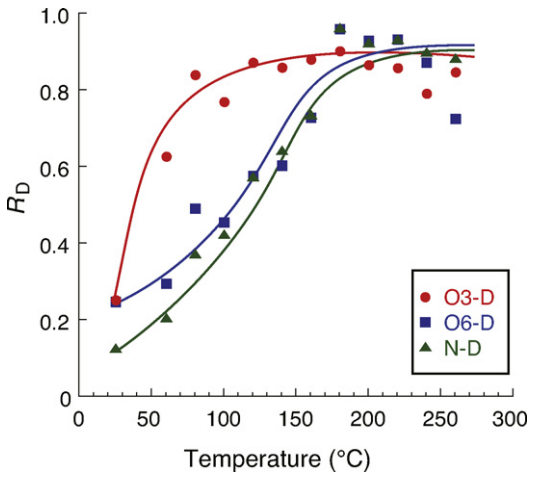

Fig. 8. Changes in the ratio of deuterium/hydrogen, R_D, of each functional group of β-chitin, with temperature.

thermodynamic stability of β-chitin is less than that of α-chitin, so it is plausible that degradation of β-chitin occurs at 260 °C (Jang, Kong, Jeong, Lee, & Nah, 2004).

Fig. 8 shows the changes in the R_D value for each functional group of β-chitin with increasing treatment temperature. In contrast with that seen for α-chitin, the deuteration among three functional groups changes with temperature. Deuteration of O3—H to O3—D progressed rapidly, even below 100 °C, and the R_D value reached around 0.8 at 120 °C. The value was almost constant above 120 °C. Conversely, the deuteration of O6—H and N—H groups progressed relatively slowly. The R_D values of these two groups increased gradually with temperature without any definite inflection points. The values reached around 0.8 at 180 °C, and were almost constant above this temperature. Therefore, almost all the O6—H and N—H in the crystal became accessible at 180 °C. Above this temperature, all the functional groups in β-chitin may become accessible, as found for α-chitin (Fig. 5).

The differences in deuteration among the three functional groups are probably associated with the geometric conditions of the functional groups and the guest D_2O molecules in the dihydrate β-chitin. The efficient deuteration of the O3—H group at low temperatures indicates the close proximity of O3—H groups to D_2O molecules compared with other functional groups. By contrast, the deuteration of the N—H groups of β-chitin progressed most gradually and was similar to that for the N—H groups of α-chitin. In anhydrous β-chitin, N—H groups form strong hydrogen bonding with C═O groups in adjacent molecules within the same molecular sheet and there is no interaction with the molecules in the adjacent sheets (Fig. 1b) (Nishiyama et al., 2011). The structure of the molecular sheets is probably maintained between the anhydrous and the hydrated β-chitin crystals (Kobayashi et al., 2010; Saito et al., 2007). This sheet structure, including N—H group geometry, is also found in α-chitin (Sikorski et al., 2009). Thus, the deuteration of N—H groups indicates the stability of N—H···O═C hydrogen bonds in dihydrate β-chitin, as found for those in α-chitin. In any case, β-chitin forms a crystalline complex with water molecules. Conversely, the O6—H groups would be located close to the guest D_2O molecules because water molecules are thought to exist between molecular sheets in the dihydrate β-chitin. However, the accessibility did not increase rapidly with temperature. A possible explanation for the difference between O3—H and O6—H deuteration is that the distance between O6 and guest D_2O molecules is longer than that between O3 and water molecules in dihydrate β-chitin. Moreover, dihydrate β-chitin was reported to be thermodynamically unstable above 80 °C. This characteristic might be affected by the state of β-chitin hydrogen-bonding systems (Saito et al., 2000).

4. Conclusion

Deuteration of highly crystalline α- and β-chitin was conducted with vapor and liquid D_2O, and monitored by FT-IR spectroscopy. The deuteration of α-chitin in vapor only progressed on the surface molecules of crystalline microfibrils at room temperature, whereas the deuteration of α-chitin with high-temperature annealing in liquid D_2O progressed within the crystallites. The deuteration was similar between each α-chitin functional group. The ratio of deuterium/hydrogen R_D increased with increasing temperature and all of the functional groups of α-chitin could be deuterated above approximately 200 °C. On the other hand, the deuteration of β-chitin is more specific for each functional group. With exposure to D_2O vapor at 25 °C, intracrystalline deuteration progressed partially on both hydroxyl groups, O3—H and O6—H, in contrast to N—H groups, which were barely deuterated. With the annealing in D_2O, intracrystalline deuteration of O3—H groups progressed even below 100 °C. The deuteration of O6—H and N—H groups on the inner part of crystallites also progressed with the annealing, but the R_D value increased relatively gradually. These differences in deuteration for each functional group of β-chitin probably arise from their geometric relationships with water molecules in hydrated β-chitin, where the deuteration progressed. From an analysis of the deuteration, we can speculate on the states of each functional group in the hydrated β-chitin.

In this study we devised the experimental method for intracrystalline deuteration of chitin polymorphs. This technique should be useful for the crystal structure analysis of chitin with the neutron diffraction method, and also applicable to the accessibility measurement of various chitin crystals.

Acknowledgments

We thank the Japan Agency for Marine-Earth Science and Technology (JAMSTEC) for collecting samples of *L. satsuma* using a remotely operated vehicle, Hyper-Dolphin. This study was supported in part by a Grant-in-Aid for Scientific Research (No. 19380097) and a Grant-in-Aid for JSPS fellows (No. 23-2362).

References

Alexander, L. E. (1979). X-ray diffraction methods. In E. Robert (Ed.), *Polymer science* (pp. 423–424). New York: Kreiger Publishing Co.

Blackwell, J. (1969). Structure of β-chitin or biopolymers, or parallel chain systems of poly-β-(1 → 4)-N-acetyl-D-glucosamine. *Biopolymers*, *7*, 281–298.

Focher, B., Naggi, A., Torri, G., Cosani, A., & Terbojevich, M. (1992). structural differences between chitin polymorphs and their precipitates from solution – evidence from CP-MAS ^{13}C NMR, FT-IR and FT-Raman spectroscopy. *Carbohydrate Polymers*, *17*, 97–102.

Frilette, V. J., Hanle, J., & Mark, H. (1948). Rate of exchange of cellulose with heavy water. *Journal of the American Chemical Society*, *70*, 1107–1113.

Gardner, K. H., & Blackwell, J. (1975). Refinement of the structure of β-chitin. *Biopolymers*, *14*, 1581–1595.

Hori, R., & Wada, M. (2005). The thermal expansion of wood cellulose crystals. *Cellulose*, *12*, 479–484.

Horikawa, Y., & Sugiyama, J. (2008). Accessibility and size of *Valonia* cellulose microfibril studied by combined deuteration/rehydrogenation and FTIR technique. *Cellulose*, *15*, 419–424.

Jang, M.-K., Kong, B.-G., Jeong, Y.-L., Lee, C. H., & Nah, J.-W. (2004). Physicochemical characterization of α-chitin, β-chitin, and γ-chitin separated from natural resources. *Journal of Polymer Science Part A: Polymer Chemistry*, *42*, 3423–3432.

Jefferies, R. (1963). An infra-red study of the deuteration of cellulose and cellulose derivatives. *Polymer*, *4*, 375–389.

Kobayashi, K., Kimura, S., Togawa, E., & Wada, M. (2010). Crystal transition between hydrate and anhydrous β-chitin monitored by synchrotron X-ray fiber diffraction. *Carbohydrate Polymers*, *79*, 882–889.

Kokot, S., Czamik-Mautusewicz, B., & Ozaki, Y. (2002). Two-dimensional correlation spectroscopy and principal component analysis studies of temperature-dependent IR spectra of cotton–cellulose. *Biopolymers*, *67*, 456–489.

Langan, P., Nishiyama, Y., & Chanzy, H. (1999). A revised structure and hydrogen-bonding system in cellulose II from a neutron fiber diffraction analysis. *Journal of the American Chemical Society*, *121*, 9940–9946.
Mann, J., & Marrinan, H. J. (1956a). The reaction between cellulose and heavy water, Part 1. *Transactions of the Faraday Society*, *52*, 481–486.
Mann, J., & Marrinan, H. J. (1956b). The reaction between cellulose and heavy water, Part 3. *Transactions of the Faraday Society*, *52*, 492–497.
Marrinan, H. J., & Mann, J. (1956). Infrared spectra of the crystalline modifications of cellulose. *Journal of Polymer Science*, *21*, 301–311.
Minke, R., & Blackwell, J. (1978). The structure of α-chitin. *Journal of Molecular Biology*, *120*, 167–181.
Muzzarelli, R. A. A. (2011). Chitin nanostructures in living organisms. In N. Gupta (Ed.), *Chitin: Formation and diagenesis* (pp. 1–34). Dordrecht: Springer.
Nara, S., Takeo, H., & Komiya, T. (1981). Studies on the accessibility of starch by deuteration. *Starch*, *10*, 329–331.
Nishiyama, Y., Isogai, A., Okano, T., Mueller, M., & Chanzy, H. (1999). Intracrystalline deuteration of native cellulose. *Macromolecules*, *32*, 2078–2081.
Nishiyama, Y., Langan, P., & Chanzy, H. (2002). Crystal structure and hydrogen bonding system in cellulose Iβ from synchrotron X-ray and neutron fiber diffraction. *Journal of the American Chemical Society*, *124*, 9074–9082.
Nishiyama, Y., Sugiyama, J., Chanzy, H., & Langan, P. (2003). Crystal structure and hydrogen bonding system in cellulose Iα from synchrotron X-ray and neutron fiber diffraction. *Journal of the American Chemical Society*, *125*, 14300–14306.
Nishiyama, Y., Johnson, G. P., French, A. D., Forsyth, T., & Langan, P. (2008). Neuteron crystallography, molecular dynamics, and quantum mechanics studies of the nature of hydrogen bonding in cellulose Iβ. *Biomacromolecules*, *9*, 3133–3140.
Nishiyama, N., Noishiki, Y., & Wada, M. (2011). X-ray structure of anhydrous β-chitin at 1 Å resolution. *Macromolecules*, *44*, 950–957.
Noishiki, Y., Kuga, S., Wada, M., Hori, K., & Nishiyama, Y. (2004). Guest selectivity in complexation of β-chitin. *Macromolecules*, *37*, 6839–6842.
Ogawa, Y., Kimura, S., Wada, M., & Kuga, S. (2010). Crystal analysis and high-resolution imaging of microfibrillar α-chitin from *Phaeocystis*. *Journal of Structural Biology*, *171*, 111–116.
Ogawa, Y., Hori, R., Kim, U. J., & Wada, M. (2011). Elastic modulus in the crystalline region and the thermal expansion coefficients of α-chitin determined using synchrotron radiated X-ray diffraction. *Carbohydrate Polymers*, *83*, 1213–1217.
Ogawa, Y., Kimura, S., & Wada, M. (2011). Electron diffraction and high-resolution imaging on highly-crystalline β-chitin microfibril. *Journal of Structural Biology*, *176*, 83–91.
Pearson, F. G., Marchessault, R. H., & Liang, C. Y. (1960). Infrared spectra of crystalline polysaccharides. V. Chitin. *Journal of Polymer Science*, *43*, 101–116.
Rudall, K. M. (1963). The chitin/protein complexes of insect cuticles. *Advanced in Insect Physiology*, *1*, 257–313.
Saito, Y., Okano, T., Gaill, F., Chanzy, H., & Putaux, J-L. (2000). Structural data on the intra-crystalline swelling of β-chitin. *International Journal of Biological Macromolecules*, *28*, 81–88.
Saito, Y., Kumagai, H., Wada, M., & Kuga, S. (2002). Thermally reversible hydration of β-chitin. *Biomacromolecules*, *3*, 407–410.
Saito, Y., Tomotake, Y., & Shida, S. (2007). Formation of a lamellar compound by reaction of acrylic acid crystallosolvated in highly crystalline β-chitin. *Biomacromolecules*, *8*, 1064–1068.
Saito, Y., & Iwata, T. (2012). Characterization of hydroxyl groups of highly crystalline β-chitin under static tension detected by FT-IR. *Carbohydrate Polymers*, *87*, 2154–2159.
Sawada, D., Nishiyama, Y., Langan, P., Forsyth, T., Kimura, S., & Wada, M. (2012). Direct determination of the hydrogen bonding arrangement in anhydrous β-chitin by neutron fiber diffraction. *Biomacromolecules*, *13*, 288–291.
Shih, A., Yeh, S-H., Lee, S-C., & Yang, T. R. (2001). Structural differences between deuterated and hydrogenated silicon nitride/oxynitride. *Journal of Applied Physics*, *89*, 5355–5361.
Sikorski, P., Hori, R., & Wada, M. (2009). Revisit of α-chitin crystal structure using high resolution X-ray diffraction data. *Biomacromolecules*, *10*, 1100–1105.
Tadokoro, H., Seki, S., & Nitta, I. (1956). Some information on the infrared absorption spectrum of polyvinyl alcohol from deuteration and pleochroism. *Journal of Polymer Science Part A: Polymer Chemistry*, *22*, 563–566.
Tanner, S. F., Chanzy, H., Vincendon, M., Roux, J. C., & Gaill, F. (1990). High-resolution solid-state Carbon-13 nuclear magnetic resonance study of chitin. *Macromolecules*, *23*, 3576–3583.
Valentin, R., Bonelli, B., Garrone, E., Di Renzo, F., & Quingnard, F. (2007). Accessibility of functional groups of chitosan aerogel by FT-IR-monitored deuteration. *Biomacromolecules*, *8*, 3646–3650.
Wada, M., Okano, T., & Sugiyama, J. (1997). Synchrotron-radiated X-ray and neutron diffraction study of native cellulose. *Cellulose*, *4*, 221–232.
Wada, M., & Saito, Y. (2001). Lateral thermal expansion of chitin crystals. *Journal of Polymer Science Part B: Polymer Physics*, *39*, 168–174.
Wada, M. (2002). Lateral thermal expansion of cellulose Iβ and III_I polymorphs. *Journal of Polymer Science Part B: Polymer Physics*, *40*, 1095–1102.
Wada, M., Chanzy, H., Nishiyama, Y., & Langan, P. (2004). Cellulose III_I crystal structure and hydrogen bonding by synchrotron X-ray and neutron fiber diffraction. *Macromolecules*, *37*, 8548–8555.